Multidimensional Upwind Fluctuation Distribution Schemes for Scalar Time Dependent Problems. *

M.E.Hubbard

The University of Reading, Department of Mathematics,

P.O.Box 220, Whiteknight

Abstract

Some techniques for improving the accuracy of multidimensional upwind fluctuation distribution schemes for the scalar advection equation are compared. One involves the construction of a consistent Petrov-Galerkin finite element scheme which is equivalent to the fluctuation distribution scheme when mass-lumping is applied. Another uses a predictor-corrector technique to improve the approximation. In both cases monotonicity is imposed using a flux-corrected transport approach. A third method is then described which combines the second order accurate Lax-Wendroff scheme with the PSI scheme via a fluctuation redistribution step which ensures monotonicity (and which is a generalisation of the FCT approach for fluctuation distribution schemes). Furthermore, the concept of a distribution point is introduced, leading to a 'preferred direction' for the limiting procedure. Extensive numerical results are presented for each of these schemes.

1 Introduction

Over the last ten years a family of cell vertex finite volume methods for the solution of the two-dimensional scalar advection equation has evolved known as multidimensional upwind fluctuation distribution schemes [3]. For the approximation of steady state flows on unstructured triangular grids these have reached a degree of maturity whereby the multidimensional schemes reproduce most of the advantages of upwind schemes in one dimension: smooth, second order accurate solutions and rapid convergence to the steady state without the necessity for additional artificial viscosity.

Unfortunately, all of the current upwind distribution schemes are only first order accurate for time-dependent flows. Recently, this problem has been addressed with some success in [6] in which the schemes have been equated with upwind finite element algorithms, but only at the expense of inverting a full mass matrix. An alternative method, which takes the form of a predictor-corrector scheme, will be described for improving the accuracy of the approach for approximating unsteady solutions of the scalar advection equation. Both of these techniques lead to spurious oscillations in the solution close to steep gradients unless some form of limiting procedure is applied. Hence they are combined with a flux-corrected transport technique [5] to ensure monotonicity.

In this report a more sophisticated approach to enforcing monotonicity (of which flux-corrected transport is a special case) will be described which can be applied to any cell vertex fluctuation distribution scheme, such as the second order accurate Lax-Wendroff scheme [3]. The new method consists of a fluctuation *re*distribution step in which the distribution coefficients are altered to avoid the creation of new extrema by the nodal updates whilst retaining conservation.

The concept of a distribution point will be described and related to monotonicity conditions derived from the local solution. Furthermore, the equivalent equation will be used to construct a preferred direction for the movement of the distribution when the redistribution is applied. Extensive numerical results will then be presented to demonstrate the effectiveness of the new techniques.

In Section 2 the multidimensional upwind schemes currently used for solv-

ing steady state problems are described. This is followed in Sections 3 and 4 by descriptions of the consistent finite element method proposed in [6] and a predictor-corrector approach based on MacCormack's scheme. The next section describes the flux-corrected transport technique for imposing monotonicity on finite element and fluctuation distribution schemes while in Section 6 a new approach is suggested based on the notion of fluctuation redistribution. Results are presented for two time-dependent scalar advection test cases in Section 7 and some conclusions are drawn at the end.

2 A Ste dy St te Scheme

Consider the two-dimensional scalar advection equation,

$$u_t + f_x + g_y \;=\; 0 \qquad \text{or} \qquad u_t + \vec{\lambda} \cdot \vec{\nabla} u \;=\; 0 \;, \tag{2.1}$$

where $\vec{\lambda} = \left(\frac{\partial f}{\partial u}, \frac{\partial g}{\partial u}\right)^{\mathrm{T}}$ defines the advection velocity. The fluctuation associated with this equation is the cell-based quantity given by

$$\begin{aligned} \phi \;&=\; -\int\!\!\int_{\triangle} \vec{\lambda} \cdot \vec{\nabla} u \; \mathrm{d}x \, \mathrm{d}y \\ &=\; \oint_{\partial \triangle} u \, \vec{\lambda} \cdot \mathrm{d}\vec{n} \;, \end{aligned} \tag{2.2}$$

where $\vec{n}$ represents the inward pointing normal to the boundary of the cell. In many cases ϕ can be evaluated exactly under an appropriate (conservative) linearisation of the equation (2.1) [3], in which case it can be written

$$\phi \;=\; -S_{\triangle} \widehat{\vec{\lambda}} \cdot \widehat{\vec{\nabla} u} \;, \tag{2.3}$$

where $S_{\triangle}$ is the cell area and the symbol $\widehat{\cdot}$ indicates an appropriately linearised quantity. For linear advection $\vec{\lambda}$ is constant so a conservative linearisation can be constructed simply by assuming that u varies linearly over each triangle with the discrete solution values stored at the nodes and continuity across the edges [3].

The numerical scheme is constructed from a discretisation of the integrated form of (2.1) by evaluating the quantity ϕ of (2.3) within each cell and then distributing it to the nodes of the grid. Combining this technique with a simple forward Euler discretisation of the time derivative leads to an iterative update of

the nodal solution v

The fluctuations in (2.7) are defined as the limited quantities,

$$\begin{aligned} \phi_i^* &= \phi_i - L(\phi_i, -\phi_j) \ , \\ \phi_j^* &= \phi_j - L(\phi_j, -\phi_i) \ , \end{aligned} \tag{2.8}$$

where

$$\phi_i \ = \ -\frac{1}{2}\widehat{\vec{\lambda}} \cdot \vec{n}_i (u_i - u_k) \ , \quad \phi_j \ = \ -\frac{1}{2}\widehat{\vec{\lambda}} \cdot \vec{n}_j (u_j - u_k) \ , \tag{2.9}$$

in which k denotes the remaining (upstream) vertex of the triangle and L denotes the minmod limiter function,

$$L(x,y) \ = \ \frac{1}{2}(1 + \mathrm{sgn}(xy)) \frac{1}{2}(\mathrm{sgn}(x) + \mathrm{sgn}(y)) \min(|x|, |y|) \ . \tag{2.10}$$

The scheme is globally positive and therefore stable, the appropriate restriction on the time-step being

$$\Delta t \ \leq \ \frac{S_i}{\sum_{j \in \cup \triangle_i} \max\left(0, \frac{1}{2}\widehat{\vec{\lambda}^j} \cdot \vec{n}_i^j\right)} \ . \tag{2.11}$$

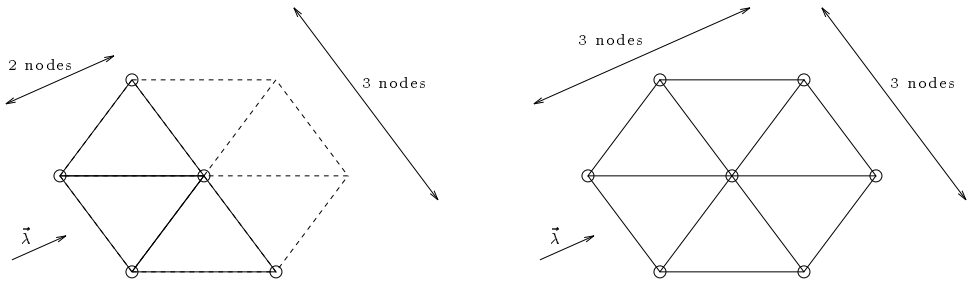

Upwind Lax-Wendroff

Figure 2.1: The stencils of the PSI scheme and the Lax-Wendroff scheme.

The above algorithm is second order accurate only at the steady state. This is not surprising since the limiter in step b) above is taking the contributions ϕ_i and ϕ_j (2.9) due to the first order N scheme [3] and redistributing the fluctuation between the two downstream vertices (along the outflow edge) which, in some sense, is giving second order accuracy in the cross-stream direction. The scheme is only first order accurate in the streamwise direction (in fact on a regular grid with edges aligned with the flow it reduces to the one-dimensional first order upwind scheme) but at the steady state this is irrelevant because the solution

is constant parallel to the streamlines. This is illustrated further in Figure 2.1 which shows the stencil of the upwind scheme and this has only two nodes in the streamwise direction.

In the following section the PSI scheme is modified to improve its accuracy for computing time varying solutions of the two-dimensional scalar advection equation on triangular grids.

2.2 Lax-Wendroff Distribution Scheme

The Lax-Wendroff scheme [3] does not have the compact stencil of the PSI scheme which allows it to attain second order accuracy. In fact it is the unique single time step second order accurate fluctuation distribution scheme on triangles with a compact stencil (as in Figure 2.1). The distribution coefficients in (2.4) which lead to this scheme are

$$\alpha_i^j = \frac{1}{3} + \frac{\Delta t}{4S_{\triangle_j}} \vec{\lambda} \cdot \vec{n}_i^j \tag{2.12}$$

where $S_{\triangle_j}$ is the area of the j^{th} cell and $\vec{n}_i^j$ is the inward pointing normal to the edge opposite node i in triangle j opposite the vertex at node i. The limit on the time-step at a node for stability of this scheme is taken as

$$\Delta t \leq 2 \min \left(\frac{4S_{\triangle_l}}{-\vec{\lambda} \cdot \vec{n}_l^j} \right) , \tag{2.13}$$

where l covers the vertex nodes in the local patch surrounding

where $K = -\vec{\lambda} \cdot \vec{\nabla} u$. Therefore, replacing S_i in (2.14) by $\sum_{\cup \triangle_i} \alpha_i^j S_{\triangle_j}$ gives the same increment at each node and hence the data remains linear at the new time level. The resulting nodal update is

$$u_i^{n+1} \;=\; u_i^n + \frac{\Delta t}{\sum_{\cup \triangle_i} \alpha_i^j S_{\triangle_j}} \sum_{\cup \triangle_i} \alpha_i^j \phi_j \;. \tag{2.15}$$

Note that this modification has no effect on the conservative nature of the distribution scheme. In fact, on regular grids in which six triangles surround each interior node the two schemes (2.4) and (2.14) are the same. It can also be shown that the area weighting of (2.14) leaves the Lax-Wendroff scheme unaltered.

3 The Finite Element Appro ch

Any fluctuation distribution scheme, such as the PSI scheme described above, can be equated with a mass-lumped Petrov-Galerkin finite element scheme, and in one dimension it is well known that using a consistent finite element formulation generally leads to a significant increase in spatial accuracy over the corresponding mass-lumped scheme. For example, applying a consistent mass matrix to the first order upwind scheme increases its spatial accuracy to third order in one dimension [6], so a similar improvement might be hoped for in the two-dimensional case.

In the previous section it was assumed that the approximate solution u was continuous and varied linearly over each triangle with the discrete values being stored at the nodes. In finite element terms this means that the solution can be written

$$u(x,y,t) \;=\; \sum_{i=1}^{N_n} u_i(t)\, \omega_i(x,y) \;, \tag{3.1}$$

where N_n is the number of grid nodes and $\omega_i(x,y)$ are the standard linear trial functions. It remains to choose the test functions so that the mass-lumped scheme is equivalent to the chosen fluctuation distribution scheme.

In [6] an SUPG-type test function is adopted. This takes the form

$$\psi_i \;=\; \omega_i + \sum_{\cup \triangle_i} \beta_i^j \kappa_j \;, \tag{3.2}$$

where κ_j takes a value of 1 on cell j and zero elsewhere, and β_i^j are coefficients corresponding to the contribution of cell j to node i and are yet to be determined.

in which i and j represent global node indices and k is the cell index. The nonzero components are easily calculated to be

$$\mathbf{M}_k \;=\; \frac{S_{\triangle_k}}{3} \begin{pmatrix} \frac{1}{2}+\alpha_1^k-\frac{1}{3} & \frac{1}{4}+\alpha_1^k-\frac{1}{3} & \frac{1}{4}+\alpha_1^k-\frac{1}{3} \\ \frac{1}{4}+\alpha_2^k-\frac{1}{3} & \frac{1}{2}+\alpha_2^k-\frac{1}{3} & \frac{1}{4}+\alpha_2^k-\frac{1}{3} \\ \frac{1}{4}+\alpha_3^k-\frac{1}{3} & \frac{1}{4}+\alpha_3^k-\frac{1}{3} & \frac{1}{2}+\alpha_3^k-\frac{1}{3} \end{pmatrix} , \qquad (3.11)$$

where α_i^k is the distribution coefficient associated with the i^{th} vertex of the k^{th} cell, so the assem

where $\underline{1}_j$ is the vector of zeros with 1 in the j^{th} entry and ϵ is a small parameter (taken here to be 10^{-10}).

When $\theta = 0$ in (3.15) the temporal discretisation is first order (forward Euler). Second order accuracy is achieved by choosing $\theta = \frac{1}{2}$ which gives a Crank-Nicolson algorithm. Note that the matrix

where $\overline{f} = f(\overline{u})$, and then to average the two updates, so that the final scheme takes the form

$$u_i^{n+1} = \frac{1}{2}(\overline{u_i} + \text{—}$$

and taking the average of the two updates gives

$$\begin{aligned} u_i^{n+1} &= \frac{1}{2}(\overline{u_i} + \overline{\overline{u_i}}) \\ &= u_i^n + \frac{\Delta t}{2S_i} \sum_{\cup \triangle_i} \left(\alpha_i^j \phi_j + \overline{\alpha_i^j} \overline{\phi_j} \right) \ . \end{aligned} \tag{4.10}$$

If the corrector step is thought of in terms of reversing the temporal discretisation then the second stage becomes

$$S_i(\overline{u_i} - \overline{\overline{u_i}}) \ = \ \Delta t \sum_{\cup \triangle_i} \overline{\alpha_i^j} \overline{\phi_j} \ , \tag{4.11}$$

and, as in one dimension, it leads to an equivalent update of

$$u_i^{n+1} \ = \ \overline{u_i} + \frac{1}{2}(u_i^n - \overline{\overline{u_i}}) \ . \tag{4.12}$$

The similarity of the predictor-corrector scheme to the two-dimensional Lax-Wendroff scheme can be illustrated by considering some simple examples of linear advection on regular grids such as those shown in Figure 4.1.

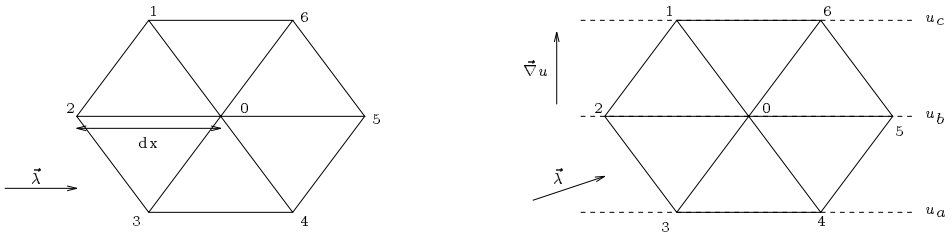

The second example shown in Figure 4.1 uses data whose gradient is perpendicular to one set of grid edges but the advection velocity is now arbitrary. The predictor-corrector scheme again reduces to a Lax-Wendroff style update, this time taking the form

$$u_i^{n+1} \;=\; u_i^n - \frac{1}{2}\nu(1-\nu)(u_c^n - u_b^n) - \frac{1}{2}\nu(1+\nu)(u_b^n - u_a^n)\;, \tag{4.15}$$

where now

$$\nu \;=\; \frac{\vec{\lambda}\cdot\vec{n}_{20}\Delta t}{S_0} \;=\; \frac{|\vec{\lambda}|\cos\theta\Delta t}{dx}\;, \tag{4.16}$$

and θ is the angle between $\vec{\lambda}$ and $\vec{\nabla}u$. In this case the two-dimensional Lax-Wendroff scheme of (2.12), also reduces to (4.15) while each of the fully upwind schemes leads to a form of first order upwinding, *i.e.*

$$u_i^{n+1} \;=\; u_i^n - \nu(u_b^n - u_a^n)\;, \tag{4.17}$$

in which ν is as in (4.16).

4.1 A Single Step Scheme

The above formulation does not result in a single step fluctuation distribution scheme as it did in one dimension (4.5) but it does provide hints as to how such a

whereas if only one vertex is downstream (vertex 1) then

$$\begin{aligned} \alpha_1^j &\rightarrow \frac{1}{2}(1+\nu_2)\overline{\alpha_2^j} + \frac{1}{2}(1+\nu_3)\overline{\alpha_3^j} \\ \alpha_2^j &\rightarrow \frac{1}{2}(1-\nu_2)\overline{\alpha_2^j} \\ \alpha_3^j &\rightarrow \frac{1}{2}(1-\nu_3)\overline{\alpha_3^j} \ , \end{aligned} \tag{4.19}$$

where $\nu_i = \frac{\hat{\vec{\cdot}}\vec{l}_i \, \Delta t}{S_\triangle}$ and $\vec{l}_i$ is the edge opposite vertex i taken in the downstream direction.

This scheme is still conservative since it remains true that

$$\alpha_1^j + \alpha_2^j + \alpha_3^j \ = \ 1 \quad \forall \, j \ , \tag{4.20}$$

and it reduces to the predictor-corrector scheme (and hence Lax-Wendroff) when the flow is parallel to the edges of a regular grid. Its major advantage over the two stage scheme is that of speed. However, in practice the scheme described above lacks robustness and is far less reliable than the Lax-Wendroff scheme.

5 Flux-Corrected Tr nsport Techniques

As it stands, none of the above higher order algorithms is monotonic so spurious oscillations can appear in the numerical solutions. In the case of the predictor-corrector and Lax-Wendroff sc

isolates the contribution from each individual grid cell to the nodes of the grid. An antidiffusive cell contribution is then calculated b

- Evaluate in order the quantities

$$\begin{aligned} u_i^* &= \begin{Bmatrix}\max\\ \min\end{Bmatrix} (u_i^{\mathrm{L}}, u_i^n) \\ u_T^* &= \begin{Bmatrix}\max\\ \min\end{Bmatrix} (u_1^*, u_2^*, u_3^*) \\ u_i^{\substack{\max\\ \min}} &= \begin{Bmatrix}\max\\ \min\end{Bmatrix} u_T^* \qquad \forall\, T \in \cup\triangle_i\ , \end{aligned} \tag{5.5}$$

  the last of which give the extreme values of the solution at each node i beyond which the updated solution is not allowed to go.

- Define

$$\begin{aligned} P_i^{\pm} &= \sum_{\cup\triangle_i} \begin{matrix}\max\\ \min\end{matrix} (0, \mathrm{AEC}) \\ Q_i^{\pm} &= u_i^{\substack{\max\\ \min}} - u_i^{\mathrm{L}} \end{aligned} \tag{5.6}$$

  and subsequently

$$R_i^{\pm} = \begin{cases} \min\left(1, Q_i^{\pm}/P_i^{\pm}\right) & \text{if } P_i^+ > 0,\ P_i^- < 0 \\ 0 & \text{if } P_i^{\pm} = 0\ , \end{cases} \tag{5.7}$$

  a nodal limiting factor for the antidiffusive contribution which ensures that the new solution value at node i does not violate the prescribed bounds.

- Finally calculate each element's limiting factor from the nodal values at its vertices so that

$$C_T = \min_{\text{vertices}} \begin{cases} R_i^+ & \text{if AEC} > 0 \\ R_i^- & \text{if AEC} < 0\ . \end{cases} \tag{5.8}$$

The above limiting is applied to the difference between the *element* contributions of the two underlying schemes.

In the case of the low order PSI scheme the splitting into element contributions is simple since the vector of nodal residuals $\underline{R}^n$ is assembled from the aforementioned element contributions and it is clear from (3.14) that a single component takes the form

$$R_i = \sum_{\cup\triangle_i} \alpha_i^k \phi_k = \sum_{\cup\triangle_i} R_i^k\ , \tag{5.9}$$

a simple sum of element contributions. Thus, the fact that

$$\mathbf{M}_L\, \Delta_n U$$

in which $\mathbf{M}_L$ is the lumped mass matrix and the symbol $\Delta_n(\cdot) = (\cdot)^{n+1} - (\cdot)^n$ represents a time difference, implies that the element contribution from cell k to node i can be written

$$\mathrm{LEC}_i^k \;=\; \mathbf{M}_L{}^{-1}\,(\alpha_i^k\,\phi_k)\,\underline{1}_i\;, \tag{5.11}$$

in which $\underline{1}_i$ is the zero vector with i^{th} component 1. $\mathbf{M}_L$ is a diagonal matrix so that all of the inversion operations are local.

In the predictor-corrector case, precisely the same analysis applies to the high order scheme when it is derived from the average of a forward and a backward space differencing except that the definition of the residual has changed, *cf.* (4.10). The high order element contribution is defined by

$$\mathrm{HEC}_i^k \;=\; \frac{1}{2}\mathbf{M}_L{}^{-1}\left(\alpha_i^k\,\phi_k + \overline{\alpha_i^k}\,\overline{\phi_k}\right)\underline{1}_i\;, \tag{5.12}$$

so that the antidiffusive element contribution evaluated in step 3 of the FCT algorithm is straightforward to calculate and the limiting can then be applied.

The consistent finite element scheme cannot be treated in the same manner because although it is true that

$$\mathbf{M}_C\;\Delta_n\underline{U}^{\mathrm{H}} \;=\; -\underline{R}^n\;, \tag{5.13}$$

the consistent mass matrix $\mathbf{M}_C$ is not diagonal so inverting it results in each component of the residual (5.9) ha

FCT techniques are applied to the implicit time-stepping of (3.15) in precisely the same manner. The low order scheme is once more taken to be the explicit mass-lumped PSI scheme and the high order scheme is the implicit consistent PSI scheme. The above analysis is then repeated, replacing the consistent mass matrix by the corresponding matrix for the implicit scheme, *i.e.*

$$\mathbf{M}_C \;\rightarrow\; \mathbf{M}_C + \theta\Delta t\mathbf{J}\;. \tag{5.17}$$

The residual $\underline{R}$ from which the Jacobian $\mathbf{J} = \frac{\partial \underline{R}}{\partial \underline{U}}$ is calculated has already been written in terms of element contributions in (5.9) and it follows that the element components of $\mathbf{J}$ can be assembled from the derivatives

$$\mathbf{J}^k_{i,j} \;=\; \sum_{\cup\triangle_i} \frac{\partial R^k_i}{\partial U_j} \quad \text{for} \quad j = 1, ..., N_n\;. \tag{5.18}$$

Since each residual component R^k_i depends only on the solution values at the vertices of its own cell, denoted here by the superscript k, $\mathbf{J}$ reduces to an assembly of 3×3 components in the same manner as $\mathbf{M}_C$ and the new matrix of (5.17) can thus be treated in the same way during the FCT stage of the algorithm.

6 Limiting by Fluctu tion Redistribution

FCT has proved to be an extremely successful technique for limiting fluxes to impose monotonicity but a loss of accuracy relative to the high order scheme, particularly noticeable when checking the error in the L_∞ norm, is unavoidable at turning points in the solution. In the fluctuation distribution framework a far more flexible technique for imposing accuracy is to redistribute the fluctuation as distributed initially by the high order scheme.

The Lax-Wendroff scheme, as given by (2.12), is a single step fluctuation distribution scheme and it is possible to combine it with the PSI scheme via redistribution to ensure monotonicity with a minimal loss of accuracy(6TnGm`` when c

6.1 The Distribution Point

A useful geometric interpretation of fluctuation distribution schemes is given by the concept of a distribution point. Consider a single grid cell in isolation: the distribution point is defined to be the point whose local area coordinates are the distribution coefficients for that triangle. Unless stated otherwise, it will be assumed from now on that the distribution coefficients are non-negative (true for both the Lax-Wendroff and PSI schemes) so that the distribution point is within the cell. Figure 6.1 shows typical distribution points for the two schemes which will be considered in this section. Note that the distribution point will lie on the outflow edge (or at the downstream vertex of a cell with one inflow edge) of the triangle when the scheme is fully upwind.

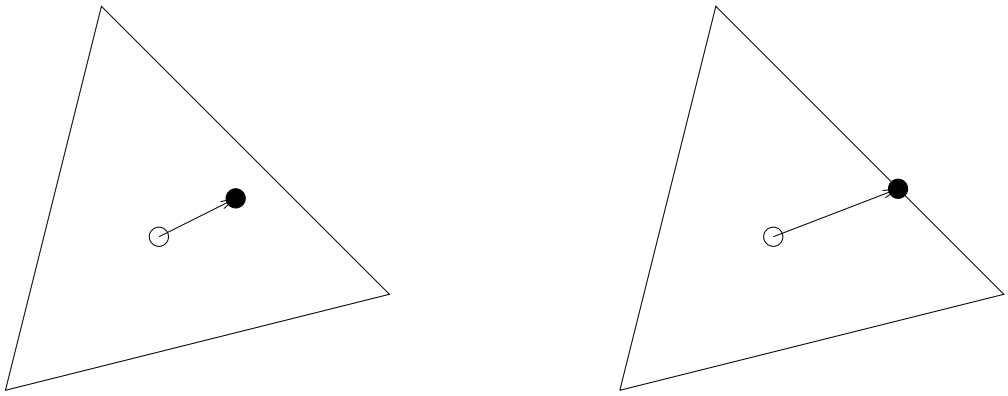

It is useful to note that the movement of the distribution point is equivalent to the *re*distribution of the fluctuation within the triangle. Furthermore, moving the distribution point parallel to an edge is equivalent to keeping the proportion of the fluctuation being sent to the opposite vertex constant, *i.e.* the redistribution is taking place between the two nodes on that edge.

6.2 The Equivalent Equation

The diffusion vector $\vec{d}$ labelled in Figure 6.1 represents the displacement of the distribution point from the centroid of the triangle (the distribution point of a symmetric central scheme). It can easily be shown by geometric arguments that the distribution coefficients of any scheme defined locally by the diffusion vector $\vec{d}$ are given by

$$\alpha_i^j \;=\; \frac{1}{3} + \frac{1}{2S_{\triangle_j}} \vec{d} \cdot \vec{n}_i^j \;. \tag{6.3}$$

The relationship with the Lax-Wendroff scheme is obvious and comparison with (2.12) immediately gives

$$\vec{d} \;=\; \frac{\vec{\lambda}\Delta t}{2} \tag{6.4}$$

in this case, as noted in Figure 6.1.

Further, a scheme with diffusion vector $\vec{d}$ can be shown [9] to have the second order equivalent equation

$$u_t + \vec{\lambda} \cdot \vec{\nabla} u \;=\; \vec{d} \cdot \vec{\nabla} (\vec{\lambda} \cdot \vec{\nabla} u) \;, \tag{6.5}$$

in which the right hand side represents the numerical diffusion of the distribution scheme and can be used to analyse the accuracy of the method.

The diffusion vector of the Lax-Wendroff scheme (6.4) can be introduced into the equivalent equation by rewriting (6.5) as

$$u_t + \vec{\lambda} \cdot \vec{\nabla} u \;=\; \frac{\vec{\lambda}\Delta t}{2} \cdot \vec{\nabla} (\vec{\lambda} \cdot \vec{\nabla} u) + \left(\vec{d} - \vec{\lambda}

Hence, any choice of $\vec{d}$ such that

$$\vec{d} - \frac{\vec{\lambda}\Delta t}{2} \perp \vec{\nabla}(\vec{\lambda}\cdot\vec{\nabla}u) \tag{6.7}$$

will not alter the second order error term in the approximation, so the corresponding distribution scheme should be second order accurate for the given local data. Therefore, moving the distribution point perpendicular to the local value of $\vec{\nabla}(\vec{\lambda}\cdot\vec{\nabla}u)$ should not change the order of accuracy of the local approximation.

It is important to note here that the second order derivative in (6.7) can be approximated locally by a first order derivative since

$$\vec{\nabla}(\vec{\lambda}\cdot\vec{\nabla}u) = \vec{\nabla}u_t \tag{6.8}$$

and u_t can be approximated simply from the unlimited high order update using

$$\vec{\nabla}u_t = \frac{1}{\Delta t}(\vec{\nabla}u^{n+1} - \vec{\nabla}u^n)\,. \tag{6.9}$$

This avoids calculating the second order spatial derivative that appears in (6.7) directly and the overall algorithm remains compact since it still involves only local operations.

6.3 The Monotonicity Region

One of the stages of the FCT algorithm of Section 5 involves constructing bounds on the antidiffusive element contributions to the cell vertices. In (5.8) the bound for a cell is taken to be the most restrictive of those at its three vertices. However, in the context of fluctuation distribution schemes this is not necessary and separate bounds can be considered at each vertex. Thus, in the notation of (5.8),

$$C_T^k = \min_{\text{vertices}} \begin{cases} R_i^+ & \text{if AEC} > 0 \\ R_i^- & \text{if AEC} < 0\,, \end{cases} \tag{6.10}$$

where node i corresponds to vertex k of triangle T. These bounds can be used to construct a monotonicity region within each triangle, an example of which is shown in Figure 6.2.

By considering a general FCT-type algorithm, in which the monotonic scheme is written in terms of low order (LO) and high order (HO) updates, the distribu-

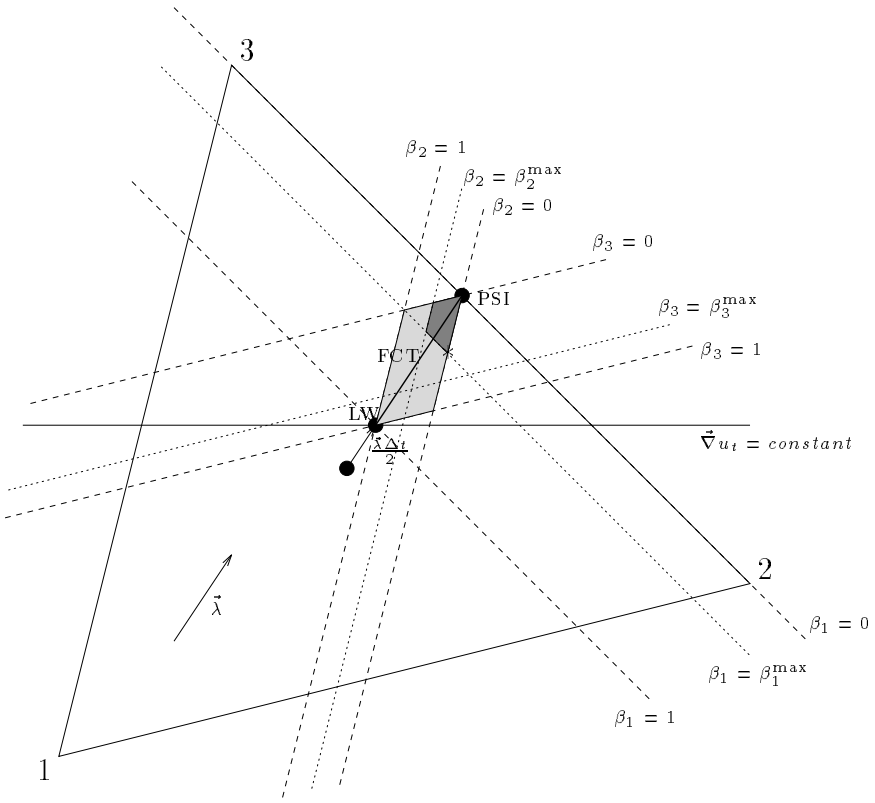

Figure 6.2: A monotonicity region for the distribution point based on the PSI and Lax-Wendroff schemes.

passing through the low order distribution point while $\beta = 1$ corresponds to the parallel line through the high order distribution point. The aforementioned linear

The path along which the distribution point travels is dictated by the 'preferred direction' (perpendicular to $\vec{\nabla} u_t$) which is suggested by (6.6). Given that the dominant error term of the scheme is proportional to some approximation to

$$\left(\vec{d} - \frac{\vec{\lambda} \Delta t}{2} \right)$$

given by the double sine wave function

$$u \;=\; \sin(2\pi x)\sin(2\pi y)\;, \tag{7.1}$$

with velocity $\vec{\lambda} = (1,1)^T$ over the domain $[0,1] \times [0,1]$. This problem has been solved on three types of grid each of which is illustrated in Figure 7.1. Periodic boundary conditions are applied.

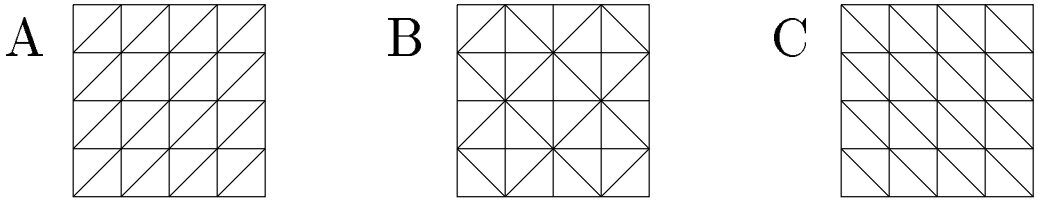

Figure 7.1: The three grid types used for the numerical experiments.

Figure 7.2 shows two solutions to the above problem obtained on a 64×64 type B grid, one obtained using the standard PSI scheme, (2.6) and (2.7), and the second including the area weighting of the nodal updates described in Section 2.3. Not only does the area weighted scheme advect the shape of the initial profile much better but the resulting solution is also slightly smoother. Further evidence of this improvement in accuracy, particularly in the L_∞ norm, is provided in Table 1 which shows the errors in the solution at $t = 1.0$ and compares them with the Lax-Wendroff scheme of (2.12). As expected the last of these is by far the most accurate since it is one order of accuracy higher than the other two.

carried out for each of the schemes under consideration and the results for the double sine wave test case described above are shown in Figure 7.3. dt/dx takes the value of 0.08 throughout for this test case.

Error estimates in the L_2 norm for the solution when $t = 1$ are shown for five different schemes. The errors in the L_1 and L_∞ norms showed very similar beha

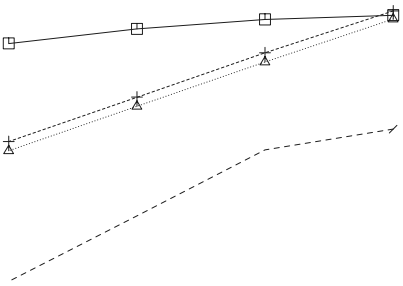

test case. It involves the circular advection of the 'cone' given by the initial conditions

$$u = \begin{cases} \cos^2(2\pi r) & \text{for } r \leq 0.25 \\ 0 & \text{otherwise} \end{cases} \tag{7.2}$$

where $r^2 = (x + 0.5)^2 + y^2$, with velocity $\vec{\lambda} = (-2\pi y, 2\pi x)^T$ around the domain $[-1, 1] \times [-1, 1]$, the solution being continually set to zero at each of the inflow boundaries. The initial profile should be advected in a circle without change of shape until it returns to its original position when $t = 1.0$.

In the numerical experiments the ratio $dt/dx = 0.04$. Three solution profiles obtained on a 64×64 type B grid are shown in Figures 7.4 and 7.5 using the schemes *without* limiters being applied. After one revolution the PSI scheme has reduced the height of the peak from 1.0 to 0.32 and is extremely diffusive, particularly in the streamwise direction. The Lax-Wendroff scheme keeps the height of the peak at 0.82 but oscillations are obvious in the wake of the cone so that some form of limiting procedure is clearly necessary. Less clear is a small phase lag which positions the peak slightly downstream of its correct position. Qualitatively, the predictor-corrector scheme gives very similar results, a small phase lag with downstream oscillations. From now on only the Lax-W

are compared with the cell-centre upwind MLG scheme [2], Figure 7.7, which is also monotonic but the peak value here is only 0.62 after one revolution. It should be noted, though, that the cell-centre scheme performs considerably better on grids of type A or C and is then comparable with the limited Lax-Wendroff scheme.

The practical order of accuracy of the monotonic schemes can be investigated using the double sine wave test case. Table 3 shows error estimates which are typical of the test case. The monotonicity constraint has little effect on the error approximations in the L_1 and L_2 norms but the fluctuation redistribution technique is significantly better than a standard FCT approach when the L_∞ norm is considered although some loss of accuracy is still incurred.

Scheme	L_1	L_2	L_∞	Peak value
Lax-Wendroff	0.0131	0.0143	0.0215	0.998
Lax-Wendroff + FCT	0.0132	0.0144	0.0263	0.996
Lax-Wendroff + FR	0.0129	0.0143	0.0230	0.998
Consistent PSI	0.0009	0.0011	0.0041	0.999
Consistent PSI + FCT	0.0010	0.0015	0.0124	0.994

Table 3: Error norms of solutions to the double sine wave problem at $t = 1.0$ on a 64×64 type B grid.

The effectiveness of the new method is also illustrated in Figure 7.8, particularly on the finer grids. The fluctuation redistribution scheme remains close to the unlimited Lax-Wendroff scheme on each of the grids while the FCT solution deteriorates on the finer grids for both the Lax-Wendroff and consistent PSI schemes. It is interesting to note that the numerical order of accuracy in the L_∞ norm on the finest grid is 2.0 for the Lax-Wendroff scheme with or without fluctuation redistribution, but reduces to 1.28 when FCT is used, while FCT reduces the order of accuracy of the consistent PSI scheme from 1.57 to 0.97. In the L_1 and L_2 norms little difference is detected in the error from that of the non-monotonic scheme on any of the grids, although typically fluctuation redistribution is more accurate than FCT on the finer grids.

1.00
0.75
0.50
u
0.25
0.00
−0.25

Finally, the schemes ha

[8], although it remains to completely overcome the lack of robustness of these extensions near to stagnation points.

Acknowledgements

The authors would like to thank Prof. M. J. Baines for his contributions to this work, Dr Nick Birkett for supplying the subroutines for the GMRES algorithm and the EPSRC for providing the funding for the first author.

[9] P.L.Roe, 'Geometry of fluctuation-splitting schemes', unpublished.

[10] Y.Saad, 'Krylov subspace techniques, conjugate gradients, preconditioning and sparse matrix solvers', *Computational Fluid ynamics*, number 1994–05 in VKI Lecture Series, 1994.

[11] Y.Saad and M.Schultz, 'GMRES: a generalised minimum residual algorithm for resolving nonsymmetric linear systems', *IAM J. cientific and tat. Comp.*, **7**:856–869, 1986.

[12] S.T.Zalesak, 'Fully multidimensional flux-corrected transport algorithms for fluids', *J. Comput. Phys.*, **31**:335–362, 1979.